

## PHASE CLOSURE NULLING: THEORY AND PRACTICE

A. Chelli,<sup>1</sup> G. Duvert,<sup>1</sup> F. Malbet,<sup>1</sup> and P. Kern<sup>1</sup>

### RESUMEN

Derivamos una teoría completa del cierre de fase en un sistema binario en el cual una compañera no detectada, muy pequeña y débil actúa como un parámetro de perturbaciones en el espectro espacial de frecuencias de una fuente dominante, intensa y resuelta. Demostramos que la influencia de la compañera puede ser evaluada con precisión midiendo el cierre de fase del sistema cerca de los ceros de la función de visibilidad primaria. En estas regiones de *ceros del cierre de fase* siempre existen intervalos de frecuencia donde el cierre de fase de la compañera *es mayor que cualquier error sistemático* permitiendo su medición. Mostramos que ésta técnica permite recobrar varias propiedades astrofísicamente relevantes de compañeras muy débiles y cercanas como son el flujo, la posición y en los casos más favorables, el espectro. Como prueba del concepto detectamos a la compañera cinco magnitudes más débil de la estrella HD-59717, a solo 3.5 radios estelares de la primaria utilizando el instrumento AMBER/VLTI con 3 telescopios auxiliares de 1.8 m en solo 15 minutos de integración en el cielo. Este es uno de los contrastes más altos detectados por la interferometría entre una compañera y su estrella principal. Concluimos con un rápido estudio del potencial de las observaciones en los ceros del cierre de fase con los interferómetros existentes y exploramos los requerimientos para un nuevo tipo de instrumento específico.

### ABSTRACT

We provide a complete theory of the phase closure of a binary system in which a small, feeble, and unresolved companion acts as a perturbing parameter on the spatial frequency spectrum of a dominant, bright, resolved source. We demonstrate that the influence of the companion can be measured with precision by measuring the phase closure of the system near the nulls of the primary visibility function. In these regions of *phase closure nulling*, frequency intervals always exist where the phase closure signature of the companion *is larger than any systematic error* and can thus be measured. We show that this technique allows retrieval of many astrophysically relevant properties of faint and close companions such as flux, position, and in favorable cases, spectrum. As a proof of concept, using the AMBER/VLTI instrument with 3 auxiliary telescopes of 1.8 m and only 15 minutes of on-sky integration, we detected the five magnitudes fainter companion of HD 59717 at only 3.5 stellar radii distance from the primary. This is one of the highest contrast detected by interferometry between a companion and its parent star. We conclude by a rapid study of the potentialities of phase closure nulling observations with current interferometers and explore the requirements for a new type of dedicated instrument.

*Key Words:* binaries: spectroscopic — instrumentation: interferometers — stars: fundamental parameters — stars: individual (HD59717) — techniques: interferometric

### 1. INTRODUCTION

The interest in all techniques related to binary size and mass estimates is reviewed by the first discoveries of low-mass companions to stars, ranging from brown dwarf to exoplanets. This opens a new challenge to measure accurately the masses and spectra of these companions. Imaging the close environment of stars is a very active research field (Marois et al. 2008; Kalas et al. 2008), and the main motivation for several ambitious instruments proposed

recently (Cockell et al. 2009; Lawson et al. 2008), based either on fringe nulling (Bracewell 1978; Woolf & Angel 1998) or “extreme” adaptive optics and coronagraphy (see review by Beuzit et al. 2007). These techniques are complementary with interferometric imaging since they are blind to regions within a couple of Airy disks from the central star, whereas the interferometric observables acquired by spatially-filtered interferometers largely come from within this Airy disk.

Ground-based optical long baseline interferometers also have potentially the capability of detecting extrasolar planets restricted to the case of a gi-

<sup>1</sup>Université Joseph Fourier, Grenoble 1/CNRS, Laboratoire d’Astrophysique de Grenoble, UMR 5571, BP 53, 38041 Grenoble Cedex 09, France (Alain.Chelli@obs.ujf-grenoble.fr).

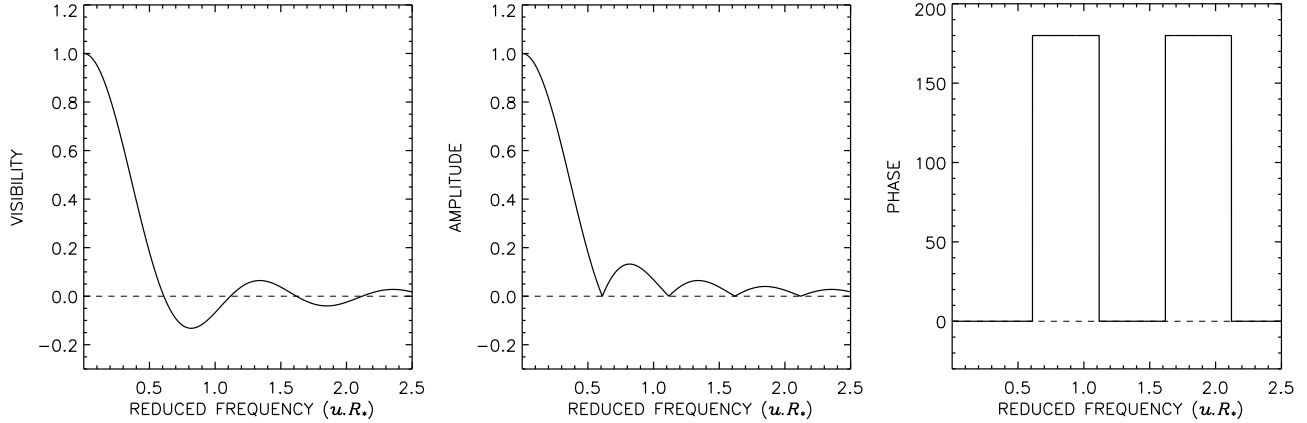


Fig. 1. Visibility for a star well represented by a uniform brightness distribution over a disk of angular radius  $R_*$  (left panel), as a function of the reduced frequency (defined as the frequency times the stellar radius). The visibility is often presented under the form of amplitude (center panel) and phase (right panel).

ant planet orbiting close to its parent stars (Vannier et al. 2006), such as 51 Peg the first exoplanet to be unraveled by radial velocity techniques (Mayor & Queloz 1995). The principle consists in measuring the interferogram phase shift as a function of the wavelength. However, even when using color-differential techniques the phase is plagued by the variation of the refractive index of air. This is why efforts are currently concentrated on using the phase closure, which corresponds to the sum of the phases measured in three connected baselines. This technique allows the observer to remove any atmospheric perturbation or instrumental-based errors localized in each arm of the interferometer.

An important property of stars resolved by long baseline interferometry is that the coherence of the light decreases with increasing spatial frequencies down to zero before increasing again following the well known behavior of the Bessel functions. Michelson & Pease (1921) used this property to measure the diameter of Betelgeuse for the first time. Indeed, the visibility of a photosphere of uniform brightness distribution over a circular disk is canceled out at the spatial frequency  $0.61/R_*$  where  $R_*$  is the stellar angular radius. Another property is that the phase of the visibility jumps by 180 degrees at each crossing of the Bessel function's zeros (hereafter called visibility nulls or simply nulls). At each null, the coherent flux of the star is canceled out, making it easier to detect a change in the phase jump due to a faint close companion.

The phase closure nulling technique (Chelli et al. 2009a) is described in § 2, its performances are discussed in § 3 and the results obtained on HD 59717 (Duvert et al. 2009) are presented in § 4. We con-

clude by a rapid study of the potentialities of phase closure nulling observations with current interferometers and explore the requirements for a new type of dedicated instrument.

## 2. PHASE CLOSURE NULLING

A multi aperture interferometer provides informations on the spatial structure of astronomical sources by measuring the object complex visibility as a function of the spatial frequency  $u = B/\lambda$ , defined as the ratio between the baseline  $B$  and the wavelength  $\lambda$ . Thanks to the Zernike-Van Cittert theorem, it can be shown that the complex visibility coincides with the Fourier transform of the object spatial brightness distribution. For a star well represented by a uniform disk of radius  $R_*$ , the visibility is proportional to a Bessel function of the first order, that is:

$$V_*(u) = 2 \frac{J_1(2\pi u R_*)}{2\pi u R_*}. \quad (1)$$

In the special case of the centro-symmetric star, the visibility turns out to be real. It is positive up to the first visibility null located at the frequency  $u_0 = 0.61\lambda/R_*$  and changes of sign at each null. The visibility can be described in terms of amplitude and phase as shown in Figure 1.

If one adds a faint unresolved companion to the previous star, assuming for simplicity that the system orientation is parallel to the frequency axis, the visibility becomes:

$$\hat{v}(u) = \frac{V_*(u) + r e^{i 2\pi u s}}{1 + r}, \quad (2)$$

where  $r$  is the flux ratio and  $s$  is the separation between the two components. For small flux ratios  $r$ ,

the amplitude of the visibility is only slightly modified by the presence of the companion. The stronger effect occurs around visibility nulls of the primary where the visibility perturbation is of the order of  $r$ . This effect remains weak and is beyond the performances of current interferometers as soon as the flux ratio is smaller than 1%.

More interesting is the phase of the object visibility. The tangent of the phase of the previous system is given by:

$$\tan \phi(u) = \frac{r \sin(2\pi us)}{V_*(u) + r \cos(2\pi us)}. \quad (3)$$

The phase is the result of two contributions: from the star  $V_*(u)$  and from the companion  $re^{2i\pi us}$ . Except around visibility nulls of the primary, that is, most of the time, the companion produces a phase signature in the range  $\pm r/V_*(u)$ , which remains small. However, around visibility nulls, in the frequency ranges for which  $|V_*(u)| \leq r$ , the phase signature of the companion becomes significant, with an exact value of  $2\pi u_0 s$  at the frequencies  $u_0$  of the nulls ( $\approx \pi s/R_*$  for the first null), much greater than 180 degrees. It follows that, as opposed to the visibility amplitude, even for small flux ratio, there is always a frequency interval around nulls within which the phase signature of the companion is larger than any systematic error and is thus measurable. However, the absolute phase of an interferogram is a quantity difficult to measure as it requires an absolute reference that in general does not exist.

Even more interesting than the phase is the phase closure. An interferometer formed by 3 telescopes transmits one phase closure  $\phi_c$  defined as the phase of the bispectrum  $\hat{I}(u_{12}, u_{23})$ , with

$$\hat{I}(u_{12}, u_{23}) = \langle \hat{i}(u_{12})\hat{i}(u_{23})\hat{i}(u_{13}^*) \rangle \quad (4)$$

where  $u_{12}$ ,  $u_{23}$  and  $u_{13}$  are the 3 frequencies transmitted by the interferometer with  $u_{13} = u_{12} + u_{23}$ , \* denotes the complex conjugate and  $\langle \rangle$  represents an ensemble average. The phase closure is a self-calibrated observable that unlike the phase does not need an absolute reference. In addition, it coincides to the phase closure of the observed object, that is:

$$\phi_c = \phi_o(u_{12}) + \phi_o(u_{23}) - \phi_o(u_{13}) \quad (5)$$

where  $\phi_o$  is the phase of the object spatial Fourier transform. Figure 2 shows the phase closure around the first visibility null of the primary, from a double system formed by an extended uniform disk and an unresolved companion with a flux ratio of 1% and various separations. Note the importance of the phase closure signature from the companion.

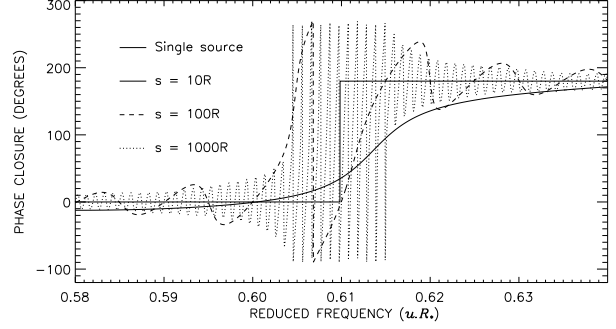


Fig. 2. Phase closure modulo  $2\pi$  of a double system, formed by an extended uniform disk and a point source, as a function of the maximum reduced frequency. The spectral resolution is  $\mathcal{R} = 1500$ . The 3 frequencies  $\{u_{23}, u_{12}, u_{13}\}$  (see equation 4) have been chosen in the ratio 1,2,3, with the maximum frequency around the first zero of visibility of the primary star. The phase closure (Duvert et al. 2009) is displayed for 3 separations ( $10 R_*$ ,  $100 R_*$ , and  $1000 R_*$ ) and a flux ratio of 0.01. The signature of the secondary source is dominant in the region around the minimum visibility of the primary (near reduced frequency 0.61). The thin line with a 180 degree shift at 0.61 corresponds to the phase closure of the primary alone.

### 3. SPECTROSCOPY OF CLOSE COMPANIONS

Chelli et al. (2009a) proposed using the regions around minima of visibility, where the *phase closure nulling* of the primary is effective, to detect and to characterize faint companions. By doing so, we do not cancel the stellar flux as in classical nulling experiments (Bracewell 1978), but we only cancel the stellar coherent flux. The main limiting noise will then be the photon noise from the central star.

The spectroscopy of close companions may be extracted from spectrally dispersed phase closure measurements obtained with an interferometer formed by at least 3 telescopes. The baselines should be such that the longest one corresponds to a null of the primary star in order to maximize the useful signal. As an example, an interferometer with 3 telescopes and frequencies  $\{u_{23}, u_{12}, u_{13}\}$  in the ratio 1:2:3, allowing bootstrapping, would be a very efficient system.

#### 3.1. Error analysis

The data consists of spectrally dispersed phase closure measurements performed as a function of the spatial frequency. The double system is characterized by 4 parameters: the stellar radius  $R_*$ , the flux ratio  $r$ , the separation  $s$ , and the position angle. The 4 parameters may be extracted from a modeling of the phase closure variations as a function of both the spatial frequency and the wavelength. The spectrum

of the companion is then obtained by multiplying the flux ratio by the spectrum of the primary. Assuming for simplicity that the direction of observation varies little during the experiment and that the working frequency domains are larger than  $s^{-1}$ , the error on the flux ratio and that on the separation due to photon noise are given by (Chelli et al. 2009a)

$$\sigma(r) \approx \frac{3}{\sqrt{K}} \quad (6)$$

$$\sigma(s/R_\star) \approx \frac{1}{r\sqrt{K}} \left( \frac{0.61}{\bar{u}_{\max} R_\star} \right) \quad (7)$$

where  $K$  is the total number of photoevents detected during the whole observation and  $\bar{u}_{\max}$  the average frequency of the longest baseline. Besides the error on the separation being inversely proportional to the maximum frequency, the errors are independent of the working frequency domains. This clearly reinforces the usefulness of observing around visibility nulls, where the phase closure signature of the companion is dominant. In the photon noise regime, both errors are independent of the spectral resolution  $\mathcal{R}$ , as long as the spectral averaging is performed over less than half a period  $1/2s$ . This condition provides a maximum recoverable distance imposed by the spectral resolution of

$$\frac{s_{\max}}{R_\star} \approx \mathcal{R} \times \left( \frac{0.61}{\bar{u}_{\max} R_\star} \right). \quad (8)$$

The error on the flux of the companion is  $\sigma(rK) \approx 3\sqrt{K}$ . The direct photometric detection of the companion would provide an error of  $\sqrt{rK}$ . In terms of performances, the direct detection is  $3/\sqrt{r}$  better than detection from phase closure. However, this is the price to pay because, to our knowledge, there is no other direct method than the one we propose, which is capable of detecting stellar companions within an Airy disk and at a distance from the hosting star as small as a few stellar radii.

### 3.2. Performances

The mean error on the flux ratio in the H band at  $1.65\mu\text{m}$  from a 3-telescope interferometer and an integration time of 3 hours, obtained by averaging all the spectral channels over an optical bandwidth of  $0.3\mu\text{m}$ , is plotted in Figure 3a. The upper curves correspond to 3 telescopes of 2 m, 1% transmission, and a Strehl ratio of 0.5. It roughly represents the present state of the AMBER instrument on the VLTI with Auxiliary telescopes (Petrov et al. 2007). The middle and lower curves correspond to telescopes of 2 m and 8 m, a transmission of 10%, and Strehl ratios of 0.9 and 0.5, respectively (see the caption of Figure 3 for details).

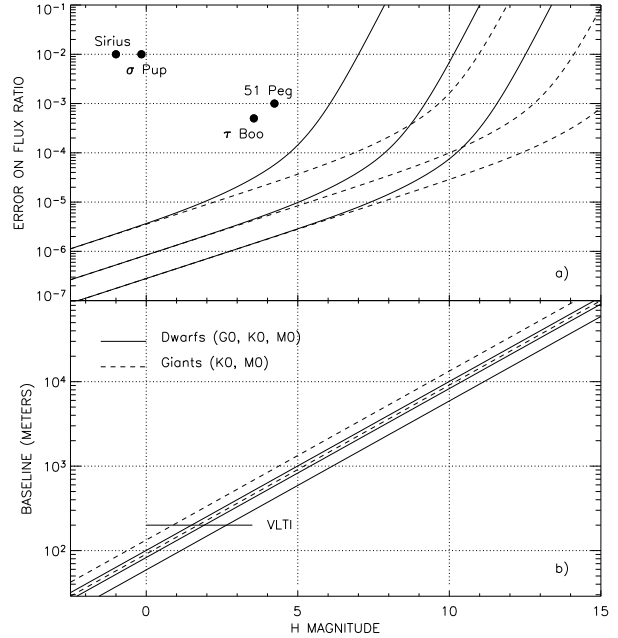


Fig. 3. (a): Error on the flux ratio of a double system from the phase closure information of a 3-telescope interferometer. The experimental parameters are; observing wavelength:  $1.65\mu\text{m}$ ; optical bandwidth:  $0.3\mu\text{m}$ ; spectral resolution: 1500; total integration time: 3 hours; integration time per frame: 0.2s; detector readout noise:  $10e^-$ ; 32 pixels per frame. The calculations took the photon noise and the detector readout noise into account. Three cases were considered: 3 telescopes with diameter  $D=2\text{m}$ , a Strehl ratio  $S=0.5$ , and 1% total transmission (upper curve, this case corresponds roughly to the present state of the AMBER experiment on the VLTI),  $D=2\text{m}$ ,  $S=0.9$  and 10% total transmission (middle curve),  $D=8\text{m}$ ,  $S=0.5$  and 10% transmission (lower curve). The broken lines correspond to an integration time per frame of 12 seconds. Represented are: Sirius with a possible M dwarf companion (Benest & Duvent 1995), the giant K5 star  $\sigma$  Puppis with its A0-4 dwarf companion (Duvert et al. 2009), and two stars with known planetary companions. (b): Baseline needed to reach the first visibility null  $1.65\mu\text{m}$  for late dwarfs and giants. The horizontal line at 200 m corresponds to the maximum baseline of the VLTI.

If we assume a signal-to-noise ratio of 10 on the flux ratio for a positive detection, then the AMBER instrument with Auxiliary telescopes would allow detection of companions  $10^4$  fainter around second-magnitude stars and  $10^3$  fainter around five-magnitude stars. Spectroscopy would be possible from flux ratios of  $10^{-4}$ . Optimized interferometers with 10% transmission (Figure 3a, middle and bottom curves) would allow the detection of companions  $10^4$  fainter around 5 to 7 magnitude stars and  $10^3$

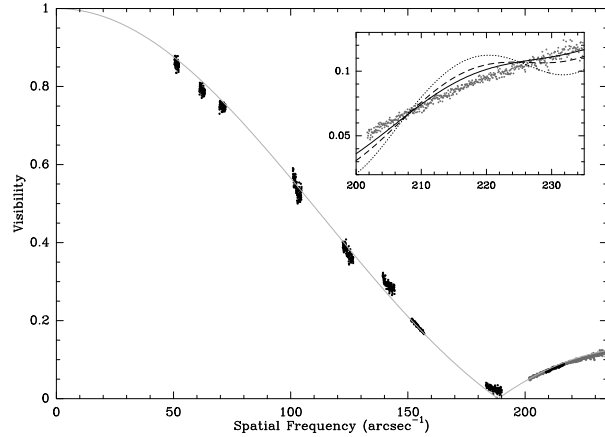


Fig. 4. Visibility of HD 59717 as a function of the spatial frequency. The full curve corresponds to a single uniform disk model of diameter 6.436 mas. The insert shows the second lobe measurements and three binary models with separation 30 mas and flux ratio:  $5 \times 10^{-3}$  (continuous line),  $1 \times 10^{-2}$  (dashed line),  $2 \times 10^{-2}$  (dotted line).

fainter around 8 to 10 magnitude stars. Spectroscopy would be possible from flux ratios of  $10^{-5}$ .

Figure 3b shows the baseline needed to resolve the primary star, that is, to reach the first visibility null for late dwarfs and giants. The horizontal line at 200 m corresponds to the maximum baseline of the VLTI, which imposes maximum H magnitudes of about 2.5 and 1.5 for M0 dwarves and giants, respectively. Also the field of view of fiber-linked interferometers is limited to one Airy disk  $\lambda/D$ , where  $D$  is the telescope diameter. Given that the baseline for reaching the first null is  $B = 0.61\lambda/R_*$ , it gives a maximum recoverable separation of about  $B/D$  stellar radii, which is 100 stellar radii on the VLTI with 2 m telescopes. A baseline of 500 m necessary for resolving a solar type star at a distance of 10 pc would provide a field of 250 stellar radii.

#### 4. APPLICATION TO THE SPECTROSCOPIC BINARY HD 59717

We illustrate the proof of concept of phase closure nulling with a simple observational case, the bright single-lined spectroscopic binary HD 59717. Although the observations were not initially intended to this purpose, and are thus very incomplete, we can nevertheless derive the characteristics of the system in terms of stellar diameter, separation and flux ratio (Duvert et al. 2009).

The observations have been performed on 13 and 14 February 2008 with the AMBER/VLTI instrument in the K band together with a spectral resolution of 1500. We used 3 auxiliary telescopes of 1.8 m

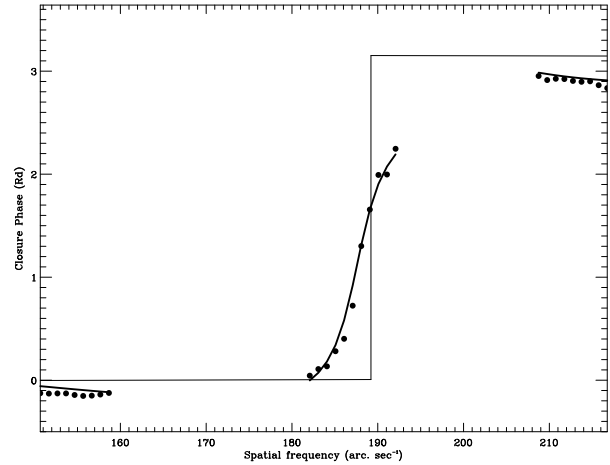


Fig. 5. Phase closure of HD 59717 as a function of the largest spatial frequency of the closure triangle. The thin curve corresponds to the best fit for a single uniform disk model with diameter 6.451 mas. The full curve corresponds to the best fit with a double system and parameters: primary stellar diameter 6.55 mas, secondary projected distance  $-11.2$  mas and flux ratio 0.017.

with baselines of 32, 64 and 96 m, in a raw east-west configuration. Due to its large angular size, HD 59717 is well resolved, the longest baseline crossing by supersynthesis effect the first zero of the visibility curve, providing information in the first and the second lobes.

#### 4.1. The data

The data have been reduced with the new AMBER data reduction software described in yChelli et al. (2009b). The calibrated visibilities of HD 59717 are shown in Figure 4 as a function of the spatial frequency. The measurements are reasonably uniformly spread over the working frequency range, with a set of measurements before, partially during, and after the minimum of visibility. The full curve represents the best fit with a single uniform disk model of diameter 6.436 mas. This is in excellent agreement with the diameter of  $6.44 \pm 0.06$  mas arising from the location of the minimum of visibility around  $189 \pm 2$  arcsec $^{-1}$ . In order to derive the parameters of the HD 59717 system, we fit the visibility with a double system formed by an extended uniform disk of radius  $R_*$  and a point source at a distance  $s$  with a flux ratio  $r$ . We find that the visibility data do not constraint well the flux ratio nor the separation. However, it provides a precise range of possible diameters for the primary:  $6.45 \pm 0.03$  mas, in agreement with the previous derivations.

The phase closure data are shown in Figure 5. The transition between the 0 and  $\pi$  values at the

zero visibility crossing is smooth, markedly different from the expected abrupt step arising from a centrally symmetric flux distribution only. The fit with a two components model does not constrain the stellar diameter of the primary because we have not the full transition, but only pieces of it. However, the slope of the transition is extremely sensitive to the flux ratio and to the separation. The possible flux ratios are in the range  $[6 \times 10^{-3}, 2.7 \times 10^{-2}]$ , which correspond to a  $5_{-0.75}^{+0.55}$  mag difference between the primary and the secondary. The permitted separations are discrete and roughly regularly spaced. The minimum flux ratio of  $6 \times 10^{-3}$  render separations larger than 30 mas irrelevant, as they would produce oscillations that are not seen on the visibility, especially in the second lobe (see insert in Figure 4). Hence, the possible projected separations left are  $-5.5$ ,  $+8.5$ ,  $-11$ ,  $+14$  and  $-17$  mas, with an error of  $\sim 1$  mas.

#### 4.2. Discussion

Although we detect the faint companion by its effect on the phase closure, the very incomplete information we have on its shape around the first null prevents a precise determination of the secondary's position using the interferometric measurements alone. It is thus important to check whether our results are in agreement with the already known spectroscopic orbit of HD 59717.

HD 59717, at a distance of 56.36 pc, has a spectroscopic period of 257<sup>d</sup>.8. The reduced mass defined by  $\mu = m_2^3 \sin^3 i / (m_1 + m_2)^2$ , where  $m_1$ ,  $m_2$  and  $i$  are the masses of the primary, that of the secondary, and the inclination angle, has been estimated by Wilson (1918) to be  $\mu = 0.164 M_\odot$ . The parameters of the photometric orbit of HD 59717, in particular the inclination  $i = 65^\circ.6 \pm 3^\circ.3$  and semimajor axis  $a_0 = 8.32 \pm 0.32$  mas, have been obtained by Jancart et al. (2005) from Hipparcos IAD measurements (van Leeuwen & Evans 1998).

In order to derive the characteristics of the HD 59717 binary system, we first combine the constraints due to our measured projected separation and the equation of mass. Figure 6 shows in black the loci of the solutions for the equation of mass with  $i = 65^\circ.6 \pm 3^\circ.3$  and  $\mu = 0.164 M_\odot$ . At the time of our observations, the position angle of the binary was  $\theta = -76^\circ.0 \pm 1^\circ.5$ , and the projection of the separation  $sp$  writes  $sp = \alpha(1 + \frac{m_1}{m_2})$ , where  $\alpha = -3.5 \pm 0.2$  is fixed by the orbit geometry. The positive projected separations ( $+8.5$  and  $+14$  mas) are forbidden by the sign of  $\alpha$ . The three possible  $(m_1, m_2)$  solutions left are for the projected separations  $-5.5$ ,

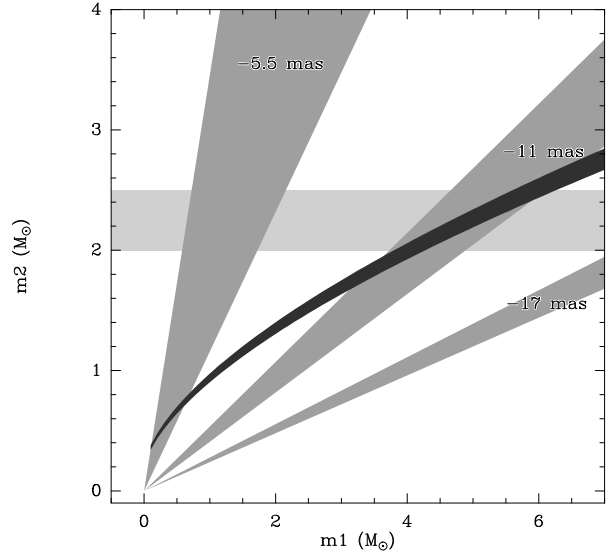


Fig. 6. Loci of the solutions for the equation of mass (black), as a function of the mass  $m_1$  of the primary and  $m_2$  of the secondary. The regions compatible with the set of 3 separations given by our fit are overlaid in gray. The region compatible with our independent measurement of the secondary's flux is overlaid in light gray.

$-11$  and  $-17$  mas, and are plotted on Figure 6 in gray. Their width correspond to the uncertainty ( $\pm 1$  mas) on the separation. The solutions for the binary masses lie at the intersection between these areas and the curve given by the equation of mass. The  $-5.5$  mas and  $-17$  mas regions give unrealistic values for the mass distribution in the binary: the former since the primary would be less massive than the secondary, the latter because it gives a too high mass for the primary. This leaves only the  $-11$  mas solution, and our mass estimate by this method is then a  $5 M_\odot$  primary and a  $2.2 M_\odot$  secondary.

If we use now the magnitude of the secondary derived from our observed flux ratio, its spectral type is A0V–A4V (see Table 1). Then  $m_2$  lies between  $2.0 M_\odot$  and  $2.5 M_\odot$  (McCluskey & Kondo 1972). In Figure 6 we have also reproduced this secondary's mass range as an horizontal area shaded in light gray. It intersects the curve of the equation of mass at  $4.5 < m_1 < 5.5 M_\odot$ , and thus gives independently the same result as our positional measurement.

Table 1 collects all the parameters on the primary that can be deduced from our size and mass measurements. We note that the radius and the mass of HD 59717 are larger than the values ( $R_{K5III} = 25 R_\odot$  and  $M_{K5III} = 1.2 M_\odot$ ) published by Schmidt-Kaler (1982). However, the masses we

TABLE 1  
 KNOWN (BOLD TEXT) AND DEDUCED PARAMETERS FOR THE A AND B  
 COMPONENTS OF THE HD 59717 BINARY

Star	mK (mag)	MK (mag)	$\Delta$ Mk (mag)	MV (mag)	$\Delta$ Mv (mag)	Sp.Type	Mass ( $M_{\odot}$ )	Radius (mas)	( $R_{\odot}$ )	$\log g/g_{\odot}$	$\log \rho/\rho_{\odot}$
A	<b>-0.41</b>	<b>-4.16</b>	-	<b>-0.55</b>	-	<b>K5III</b>	$5 \pm 0.5$	$3.23 \pm 0.015$	39	-2.5	-4.7
B	5.14	1.39	5.5	1.8	2.4	A4V	2.0	0.15	1.8	-	-
B	4.89	1.14	5.3	1.3	1.9	A2V	2.2	0.16	2.0	-	-
B	4.59	0.84	5.0	0.65	1.2	A0V	2.5	0.2	2.4	-	-

obtain are in agreement with the values ( $M_A = 5 M_{\odot}$ ,  $M_B > 1.9 M_{\odot}$ ) quoted in the MSC catalog (Tokovinin 1997) for the components of HD 59717.

## 5. DISCUSSION

### 5.1. Science cases

We have demonstrated that a phase closure nulling experiment can bring astrophysically significant information on the close environment of resolved stars. The technique is not limited to observing unbalanced binary systems but can also address a broader range of topics. These topics may change either by changing the nature of the resolved bright astrophysical target and/or the off-axis accompanying astrophysical signal.

In star and planet formation, astronomers are interested in protoplanetary disks, which in general have the property of being centro-symmetric so that the phase closure signal is zero or  $\pi$ . Any perturbing signal located off-axis can then be detected by closure phase nulling: inhomogeneities on the disk surface, presence of a forming planetesimal, presence of a collimated jet of outflowing wind partially screened by the disk. It also applies to other science cases holding disk-like cataclysmic variables, active galactic nuclei, protoplanetary nebulae, gaseous disk around hot stars. The case of exoplanets, especially hot Jupiters, is of particular interest, but the various kind of binaries must not be forgotten involving young, main sequence, or evolved stars and even the case of merging binaries.

### 5.2. Towards a dedicated instrument

We have discussed the main properties of phase closure nulling: around each null of the visibility function of the star, a spatial frequency interval exists where the signal of a companion becomes stronger than any systematic error, hence potentially detectable. The errors on the companion detection, both in flux ratio and in position, depend roughly

on the square root of the number of star photons detected, and the imageable region for a fiber-linked interferometer (the distance from the star where the companion's signature can be seen) is  $\approx B/D$  stellar radii. The need to be at a star null fixes a minimum baseline length. The need to reach a given sensitivity for the flux ratio implies either a given minimum size for the telescope apertures, thus a maximum imageable area, or/and a given integration time. The spectral resolution  $\mathcal{R}$  does not need to be very high, typically  $\approx B/D$ .

Today interferometers with baselines of a few hundred meters can already detect faint companions to the few closest giant stars using phase closure nulling. It seems possible to go further –and still use ground-based optical arrays– to characterize the faint companions, down to hot Jupiter masses, of the nearby main-sequence stars. This can be envisioned with an interferometer, that

1. Reaches the first zero of a solar-type star at 10 pc in an infrared band (kilometric baselines);
2. Has a spectral resolution of  $\approx B/D$  to enable detection of companions up to  $\approx B/D$  stellar radii. This is 500 for a 1000m baseline and 2 m-class telescopes;
3. Permits long integration times on the zero crossing thanks to earth rotation and repositionable telescopes;
4. Has the highest attainable transmission: since our S/N only depends on the photon S/N of the primary, this should be as large as possible. Since we are only interested in phase closure that is a robust measurement insensitive to relay optics wave-front disturbance or atmosphere stability, the attention should go on improving the transmission of the relay optics, not their optical quality. This is best realized with fully integrated optics, fiber linking the foci of the telescopes at the primary focus;
5. Uses a few detectors with low noise for the detection, such as a 4-pixel ABCD method. New

developments (Rothman et al. 2007) seem to imply that such low-noise IR detectors can be available in a few years from now;

6. Takes advantage of the new developments in integrated optics, permitting both beam recombination and spectrography, thus avoiding the losses at all the diopters of bulk optics used for beam transportation and in the spectrograph. Such a concept, derived from on-going developments for visible spectroscopy (Le Coarer et al. 2007) is under investigation (Kern et al. 2009) and can be envisioned on the sky in the coming few years.

## 6. CONCLUSION

We have introduced both the concept of phase closure nulling and its application in the detection of faint close companions to resolved stars, accurately measuring their position and spectra. This concept is the only one to date to permit such direct detection *inside* an Airy disk. We computed the performances of the phase closure nulling, and showed how this method permits ground-based interferometry to complement and, in favorable cases, compete with the direct detection methods considered for future space-borne experiments. We proved the feasibility of the technique detecting the companion of the spectroscopic binary HD 59717 five magnitudes fainter than the primary at only 3.5 stellar radii distance. This result, obtained with only 15 minutes of on-sky integration and 1.8 m apertures, is two magnitudes fainter than reported detection limits (applying equation A.2 of Tokovinin et al. 2006, for  $\rho = 11$  mas). At last, we discussed a few science cases that would benefit from phase closure nulling experiments and sketched the requirements for a new type of interferometer dedicated to such studies.

This research has made use of the **SearchCal** service of the Jean-Marie Mariotti Centre<sup>2</sup>, of the CDS Astronomical Databases SIMBAD and VIZIER, and of the NASA Astrophysics Data System Abstract Service.

## REFERENCES

- Benest, D., & Duvent, J. L. 1995, *A&A*, 299, 621  
 Beuzit, J.-L., Mouillet, D., Oppenheimer, B. R., & Monnier, J. D. 2007, in *Protostars and Planets V*, ed. B. Reipurth, D. Jewitt, & K. Keil (Tucson: Univ. Arizona Press), 717  
 Bracewell, R. N. 1978, *Nature*, 274, 780  
 Chelli, A., Duvert, G., Malbet, F., & Kern, P. 2009a, *A&A*, 498, 321  
 Chelli, A., Hernandez Utrera, O., & Duvert, G. 2009b, *A&A*, 502, 705  
 Cockell, C. S., et al. 2009, *Astrobiology*, 9, 1  
 Duvert, G., Chelli, A., Malbet, F., & Kern, P. 2009, *A&A*, in press  
 Jancart, S., Jorissen, A., Babusiaux, C., & Pourbaix, D. 2005, *A&A*, 442, 365  
 Kalas, P., et al. 2008, *Science*, 322, 1345  
 Kern, P., Le Coarer, E., & Benech, P. 2009, *Opt. Express*, 17, 1976  
 Lawson, P. R., et al. 2008, *Proc. SPIE*, 7013, 80  
 Le Coarer, E., et al. 2007, *Nature Photonics*, 1, 473  
 Marois, C., et al. 2008, *Science*, 322, 1348  
 Mayor, M., & Queloz, D. 1995, *Nature*, 378, 355  
 McCluskey, Jr., G. E., & Kondo, Y. 1972, *Ap&SS*, 17, 134  
 Michelson, A. A., & Pease, F. G. 1921, *ApJ*, 53, 249  
 Petrov, R. G., et al. 2007, *A&A*, 464, 1  
 Rothman, J., et al. 2007, *Proc. SPIE*, 6542, 654219  
 Schmidt-Kaler, T. 1982, *Landolt-Börnstein Numerical Data and functional Relationships in Science and Technology, New Series, Group VI, Astronomy and Astrophysics, Vol. 2B*, (Berlin: Springer)  
 Tokovinin, A., Thomas, S., Sterzik, M., & Udry, S. 2006, *A&A*, 450, 681  
 Tokovinin, A. A. 1997, *A&AS*, 124, 75  
 Traub, W. A., & Jucks, K. W. 2002, in *AGU Monograph Ser. 130, Atmospheres in the Solar System: Comparative Aeronomy*, ed. M. Mendillo, A. Nagy, & J. H. Waite (Washington, DC: American Geophysical Union), 369  
 van Leeuwen, F., & Evans, D. W. 1998, *A&AS*, 130, 157  
 Vannier, M., Petrov, R. G., Lopez, B., & Millour, F. 2006, *MNRAS*, 367, 825  
 Wilson, R. E. 1918, *Lick Obs. Bull.*, 9, 116  
 Woolf, N., & Angel, J. R. 1998, *ARA&A*, 36, 507

<sup>2</sup>Available at <http://jmmc.fr>.